

# Radio Location of Partial Discharge Sources: A Support Vector Regression Approach

E. T. Iorkyase<sup>1</sup>, C. Tachtatzis<sup>1</sup>, P. Lazaridis<sup>2</sup>, I. A. Glover<sup>2</sup>, R. C. Atkinson<sup>1</sup>

<sup>1</sup> Department of Electronic and Electrical Engineering, University of Strathclyde, Royal College Building, 204 George Street, Glasgow, G1 1XW, UK

<sup>2</sup> Department of Engineering and Technology, University of Huddersfield, HD1 3DH, Huddersfield, UK

\*[ephraim.iorkyase@strath.ac.uk](mailto:ephraim.iorkyase@strath.ac.uk)

**Abstract:** Partial discharge (PD) can provide a useful forewarning of asset failure in electricity substations. A significant proportion of assets are susceptible to PD due to incipient weakness in their dielectrics. This paper examines a low cost approach for uninterrupted monitoring of PD using a network of inexpensive radio sensors to sample the spatial patterns of PD received signal strength. Machine learning techniques are proposed for localisation of PD sources. Specifically, two models based on Support Vector Machines (SVMs) are developed: Support Vector Regression (SVR) and Least-Squares Support Vector Regression (LSSVR). These models construct an explicit regression surface in a high dimensional feature space for function estimation. Their performance is compared to that of artificial neural network (ANN) models. The results show that both SVR and LSSVR methods are superior to ANNs in accuracy. LSSVR approach is particularly recommended as practical alternative for PD source localisation due to its low complexity.

## 1. Introduction

Electrical substation assets such as transformers are known to be susceptible to partial discharge (PD). PD occurs when an electrical discharge partially bridges the dielectric between conductors; it tends to be highly focused where electric field strength is greater than the breakdown strength of the insulator. Example locations of local defects include air pockets in solid insulation, gas bubbles or particles in liquid insulation [1] [2] [3]. Regardless of the underlying cause, PD is indicative of degraded insulation. The discharges themselves further deteriorate the quality of the insulation thereby giving rise to a vicious circle of atrophy until failure [4]. Instituting a monitoring process permits PD activity to be detected at an early stage and proactive maintenance can be employed to avoid catastrophic failure of assets. Thus, unplanned outages and expensive repair costs can be significantly ameliorated.

The occurrence of partial discharge can be determined using protection equipment that monitors changes in the electric current [5]. The discharges also produce acoustic emissions [6] [7]; consequently, ultrasonic detectors have been used to determine their location. This is particularly useful in small indoor installations. Another approach is to monitor the radio spectrum for RF pulses emitted by the discharges [8] [9]; the method is more suited to larger transmission substations.

In recent past, effort towards accurate PD localization has been reported. Hou proposed a PD location method based on L-shaped array [1], which composed of four UHF omnidirectional antennas. In [4] and [10], remote radiometric technology was used to locate PD source in two-dimension (2-D). In [11] and [12], time delay method based on energy accumulation was employed to estimate the location of a PD source in three dimension (3-D). The setup

composed of four omnidirectional micro-strip antennas and four omnidirectional discrete disk-cone antennas. [13] used four omnidirectional antennas to capture the UHF signals radiated by PD and the principle of signal time delay estimate based on high order statistics to locate PD sources. In [8], omnidirectional and directional antennas were both used to locate PD source in air-insulated substation. The time-delay was computed using the cross-correlation algorithm based on wave-front. A vehicle, such as a van, furnished with the necessary equipment can be taken periodically to substations to monitor for the presence of discharge [14] [15]. In previous works, radiolocation-based approaches for localisation of PD sources used Time Difference of Arrival (TDoA)/Time Delay Estimation (TDE) and Direction of Arrival (DoA) [16] [17] [18] [19] of the RF signal as the basic principles. However, time based methods require accurate temporal synchronisation, making it expensive and complex, and hence too costly to deploy for continuous monitoring of PD. The DoA method is also complex, requiring directional antenna array. Consequently, alternative solution to network relatively low-cost sensors for continuous monitoring an entire substation are of practical interest and are being explored. The cost/complexity of other approaches prompts an investigation into methods based solely on the use of Received Signal Strength (RSS) measurements due to their simplicity, low-power consumption and cost effectiveness. Theoretical RSS-based methods require knowledge of the underlying radio propagation environment (e.g. path loss) such that a suitable propagation model that defines the relationship between RSS and distance to an antenna can be built. It is not appropriate to use a ready-made propagation model due to multipath problem that often characterise the real-life radio environments in which PD is experienced. Alternative methods based on radio fingerprinting present themselves [20] [21]. These consist of identifying radio signatures (finger prints) from discharges at known locations,

and sophisticated machine learning algorithms can be used to estimate the location of true discharge. Fingerprinting often involve a resource intensive survey stage where a new radio map (of signatures) is needed each time a change occur in the propagation environment in order to maintain the needed accuracy.

In this work we suggest a low-cost Wireless Sensor Network (WSN) approach where the network itself builds the spatial RSS map of signatures autonomously and continually. With this approach PD monitoring system can be permanently deployed and thus monitor the substation in real-time at low cost without interruption.

The key challenge of the above described PD localisation procedure is how to effectively and efficiently model RSS/location relation and hence derive PD location from RSS. The complexity of this inverse problem motivates the use of flexible models based on machine learning. This approach not only obviate the need for a propagation model but can also improve localisation precision.

The rest of this paper is organized as follows. Section 2 presents the statement of the problem. In section 3, a description of the PD localisation learning algorithms is presented. The experimental set up and data preparation procedure are addressed in section 4. The experimental results are discussed in section 5. Finally, the concluding remarks are stated in section 6.

## 2. Problem Statement

This low-cost approach is based on the deployment of wireless sensors at arbitrary but know locations in the substation compound; these sensors can record radio emission from PD sources in real-time. The locations of these sources can be inferred by sophisticated algorithms.

Due to the topography of assets in a substation, PD localisation in this setting can be regarded as a 2 dimensional problem. The compound is modelled as a finite location space  $L = \{l_1, \dots, l_n\}$  of n discrete locations where

$l_i = (l_i^x, l_i^y)$  represents the 2D coordinate of a PD source in physical space. In this paper we exploit the mathematical relationship between PD location and signal attenuation to estimate a function which provides PD source location  $l_i = (l_i^x, l_i^y)$  from measured signal strength. This can be modelled as;

$$l = f(r) + e(r) \quad (1)$$

where  $r \in R$  is the vector containing the RSS from M known locations captured by Q antennas,  $f = R_M^Q \rightarrow L$  and e accounts for the noise.

Each of the sensors take a turn at emitting a radio pulse, which is monitored by the others. Given that they are at known locations, this permits a database of to be built which implicitly characterises the radio environment of the substation. The database is defined as  $D = \{D_1, \dots, D_M\}$  with  $D_m = (r_m, l_m)$  where  $r_m = [r_m^1, \dots, r_m^Q]$  are the RSS measurement from the Q antennas at location  $l_m$ . The transmission power of a true PD source is dependent on a

great many factors and cannot be known a priori, furthermore, it increases in severity over time. Therefore, the ratio of RSS components between pairs of sensor nodes is preferred to absolute values of RSS in our model.

It is assumed that for any pair of PD sources close in the physical location space, their RSS, hence RSS ratio vectors should be similar compare to sources far away. This assumption is based on the fact that these locations may have relatively similar propagation channels and may exhibit comparable RF characteristics. Suppose  $r_i = [r_{i1}, \dots, r_{iQ}]$  and  $r_j = [r_{j1}, \dots, r_{jQ}]$  are the signal strength vectors from locations  $l_i$  and  $l_j$ . If  $\|l_i - l_j\|$  is small, then  $\|r_i - r_j\|$  should also be small.

The key challenge is to develop a model that can determine as accurate as possible the planar location of PD sources based on the location data at low cost. Both the receiving sensor nodes and the PD sources are made stationary during measurement.

## 3. Modelling ANN and SVM for PD Location

### 3.1 Artificial Neural Network

The artificial neural network (ANN) [22] approach for PD localisation is regarded as a function approximation problem consisting of a nonlinear mapping of the PD signal strength input onto dual output variables representing the location coordinates of the PD source. In this work, two variants of ANN; the multilayer perceptron (MLP) [23] [24] and the radial basis function neural network (RBFN) [25] [26] models are adopted for PD localization.

#### 3.1.1 PD Localisation Based on Multilayer Perceptron

The MLP network consists of an input layer, hidden layer(s) and an output layer. An MLP with a single hidden layer can be represented graphically as shown in Fig. 1. A sigmoidal activation function is used in the hidden layer to provide robustness against outliers and a linear activation function in the input and output layers. The MLP-type ANN is based on the back propagation [24] training of error estimate. It is generally an iterative non-linear optimisation technique. In this study, the MLP approach has been processed in two phases: a training phase and location estimation phase. During the training phase, the MLP network is trained to form a set of fingerprints as a function of PD location.

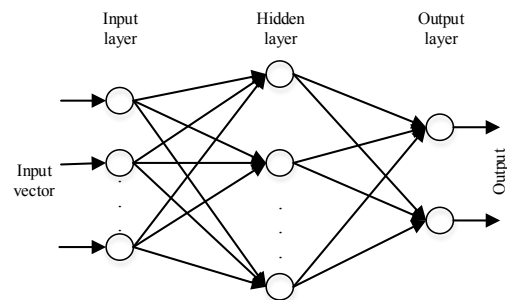
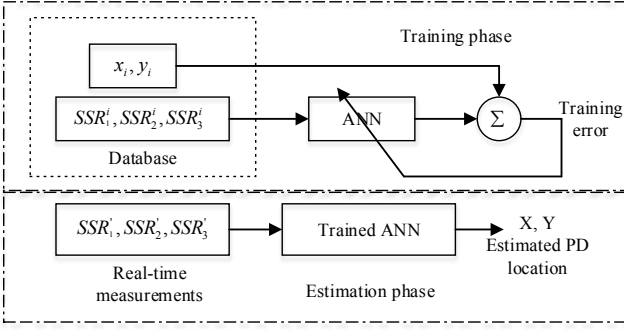


Fig. 1. MLP Architecture



**Fig. 2.** MLP model for PD localisation

A set of training examples (fingerprint (RSS) and their corresponding locations) is applied to the network to learn the relation between fingerprints and their locations. This involves tuning the values of the weights and biases of the network to optimise network performance. The batch mode training is implemented in this work. All the inputs in the training set are applied to the network before weights are adjusted to minimise the error between the network output and the desired output. The MLP model developed for PD localisation is as shown in Fig. 2.

During the estimation phase, the PD signal strength values from unknown locations are applied to the input of the trained network to give output corresponding to the PD location. To develop an appropriate MLP model for PD localisation, cross validation is used to determine a suitable network structure in terms of number of hidden neurons. The available training data is randomly partitioned into  $k$  disjointed sets. The network is trained for each set of parameters, on all the subsets except for one and the validation error is measured on the subset left out. The procedure is repeated for a total of  $k$  trials, each time using a different subset for validation. The average of MSE under validation represent the performance of the network. This process is repeated for different network architecture in terms of number of hidden neurons. The 3-4-2 network model with 3 inputs nodes, 4 hidden neurons and 2 outputs nodes has the best performance and is adopted in this work. In order to improve the generalisation of the model (that is model's ability to do well on unseen data rather than just training set) and avoid overfitting, Bayesian regularisation [23] is used to train the network.

### 3.1.2 Radial Basis Function Network Method

In general, Radial Basis Function (RBF) networks are ANNs that have single hidden layer with nonlinear radial basis function. In this work, the RBF network architecture used for PD localisation consist of three inputs, corresponding to the RSS measurement data from the three sensors, a hidden layer and an output layer with two neurons, representing PD location coordinates  $(x, y)$ . The structure of a fully connected PD localisation RBF network is as shown in Fig. 3. A radial basis type activation function (Gaussian function) is used for neurons in the hidden layer and a linear activation function for the output layer. The fully connected RBF network is used to approximate  $f = R_M^O \rightarrow L$ , a mapping of PD RSS fingerprints onto PD locations in the physical space.

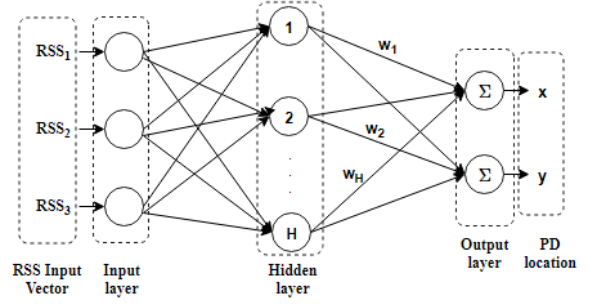


**Fig. 3.** RBFN PD localisation model

The RBF network consist of two phases: a learning phase and an estimation phase. In the learning phase, the RBF network is trained to form a set of RSS fingerprints as a function of PD location. Each fingerprint is applied to the input of the network and corresponds to the measured RSS-location data. The weights between the hidden layer and the output layer are iteratively adjusted to minimise location error. In the real-time estimation phase, measured PD RSS is applied to the input of the RBF network (acting as a pattern matching algorithm). The output of the RBF network which is the weighted sum of the radial basis function is the PD location estimate.

Given a PD fingerprint  $r'$  (RSS), the estimated location  $\hat{l}$  given by the weighted sum of Gaussian basis function [25] is

$$\hat{l}(r') = f(r') = \sum_{k=1}^H w_k u(\|r' - h_k\|) \quad (2)$$

Where  $\varphi(\|r' - h_k\|) = \exp(-\beta\|r' - h_k\|^2)$  is the Gaussian radial basis function.  $H$  is the number of neurons (basis functions) in the hidden layer which correspond to the number of training samples,  $h_k$  is the 3-dimensional center for hidden layer neuron  $k$ , and  $w_k$  are the 2-dimensional weights for the linear output layer.  $\beta$  is the spread or width of the Gaussian function. For improved performance, the normalized basis function can be used in the model. The weights can be determined in order to optimize the model. Each fingerprint defines the center of a neuron and the width  $\beta$  is obtained via cross validation. Thus, forming the following set of equations;

$$l_i = \sum_{k=1}^H w_k u(\|r(l_i, m) - h_k\|), \quad i = 1, \dots, L, \quad m = 1, \dots, M \quad (3)$$

This system of linear equations can be written in matrix form as  $Uw = d$  and the weights are easily obtained by  $w = U^{-1}d$ .  $U = \{u(\|r_j - h_i\|) | (j, i) = 1, \dots, R\}$  and  $u(\cdot)$  is the normalised Gaussian basis function. The computed weights are then used during the estimation phase to locate PD. RBF networks suffer from high memory requirements since all reference fingerprints are used as centers for the basis functions and required for localisation.

### 3.2 Support Vector Machine

Support Vector Machines (SVM) [3] [27] [28] are kernel-based learning techniques applicable to both classification and regression problems. SVMs are based on the idea of mapping the original input data point to a high dimensional feature space where a separating hyper-plane can be easily identified. SVMs have shown tremendous success in applications such as data classification, time series prediction, identification systems and data clustering [28] [29] [30] [31] [32]. In the context of PD localisation, SVM is formulated as a regression task, which consist of training a model that defines the non-linear mapping function between the PD RSS and its geo-spatial location in high dimensional feature space, leading to Support Vector Regression (SVR) [33] [34] [35].

#### 3.2.1 Support Vector Regression:

##### 3.2.1.1 Basic theory of SVR

Support vector regression technique is a learning procedure based on statistical learning theory which employs structural risk minimisation principles [33]. SVR uses training data to build its prediction model. This method can solve both linear and nonlinear regression problems. If the training samples are nonlinear, SVR maps the samples into a high-dimensional feature space by a nonlinear mapping function, where samples become linearly separable and the optimal regression surface is constructed [36].

Suppose we are given training dataset  $D = \{(r_i, l_i)\}$  with  $r_i \in \mathcal{R}$  and  $l_i = L$ , the goal of SVR is to find the mapping  $f: \mathcal{R} \rightarrow L$  and make  $f(r_i) \sim l_i$ , where  $r$  is input feature vector. For nonlinear problem, the training patterns are pre-processed by a map into some feature space before SVR is applied. SVR finds the best or optimal regression surface  $f(r)$  within a deviation  $\varepsilon$  as the prediction model, leading to epsilon-SVR [37]. The model can be expressed as

$$f(r) = \langle w, r \rangle + b, \quad w \in \mathcal{R}^n, b \in \mathcal{R} \quad (4)$$

Where  $\langle \cdot, \cdot \rangle$  denotes the dot-product and  $w$  and  $b$  are the support vector weight and bias respectively. A small  $w$  is desired to get an optimal regression surface. This can be achieved by solving the following optimisation problem with the training data  $D = [R, L]$ :

$$\begin{aligned} \min \quad & \frac{1}{2} \|w\|^2 \\ \text{subject to} \quad & \begin{cases} l_i - \langle w, r_i \rangle - b \leq \varepsilon \\ \langle w, r_i \rangle + b - l_i \leq \varepsilon \end{cases} \end{aligned} \quad (5)$$

Where  $\|w\|^2 = \langle w, w \rangle$ . The problem in (5) might be restrictive by bounding the range of errors of the training data within  $\varepsilon$ . Thus, to deal with otherwise infeasible constraints, introduce slack variables  $\xi_i, \xi_i^*$  for each point.

The slack variables allow errors to exist up to the value of  $\xi_i$  and  $\xi_i^*$  without degrading performance. With slack variables the problem becomes [38]:

$$\begin{aligned} \min \quad & \frac{1}{2} \|w\|^2 + C \sum_{i=1}^N (\xi_i + \xi_i^*) \\ \text{subject to} \quad & \begin{cases} l_i - \langle w, r_i \rangle - b \leq \varepsilon + \xi_i \\ \langle w, r_i \rangle + b - l_i \leq \varepsilon + \xi_i^* \\ \xi_i, \xi_i^* \geq 0 \end{cases} \end{aligned} \quad (6)$$

Where  $C$  is the box constraint, a positive numeric value that controls the penalty imposed on data points that lie outside the  $\varepsilon$  margin and helps to prevent overfitting (regularisation). To solve the problem in (6), a standard dualisation method with Lagrange multipliers  $\alpha_i, \alpha_i^*$  can be used [36]. By solving the dual problem,  $w$  can be expanded as

$$w = \sum_{i=1}^N (\alpha_i - \alpha_i^*) r_i \quad (7)$$

Where  $\alpha_i \geq 0$  and  $\alpha_i^* \geq 0$ . Substituting (7) in (4), and replacing the dot-product  $\langle \cdot, \cdot \rangle$  with a kernel function  $k(r_i, r)$  [38] to simplify the nonlinear mapping from the input space to the feature space in SVR, the model can be expressed as

$$f(r) = \sum_{i=1}^N (\alpha_i - \alpha_i^*) k(r_i, r) + b \quad (8)$$

$\alpha_i$  are the Lagrange multipliers which satisfy  $0 < \alpha_i^* < C$ ,  $r_i$  are the support vectors whose  $\alpha_i$  is not zero, and  $N$  is the number of support vectors. Equation (8) shows that the decision function depends on support vectors. This means optimal regression surface is constructed by these support vectors. The idea of support vectors form a sparse subset of the training data that can be used and is particularly useful for resource constraint applications such as the one under investigation.

##### 3.2.1.2 PD Localisation based on SVR

In PD localisation problem, sensors are deployed at arbitrary but known locations in a two-dimensional substation compound; these sensors record radio emission from PD sources in real-time and estimate the location of the PD. The compound is divided into a 1x1 squared grid. Each grid point represented by x-y coordinate is considered a PD location (source). Therefore, to compute PD location, two SVR models are required; one for each x-y coordinates. The PD features/patterns used to develop the SVR models is the received signal strength. Firstly, RSS from known locations are gathered by the three sensors deployed in the substation compound. These RSS and their locations form a database for the compound. Suppose the true coordinates of PD

location  $l_i$  are  $(x_i, y_i)$  and the corresponding values of RSS for the PD from this location are  $(r_i^1, r_i^2, r_i^3)$ .

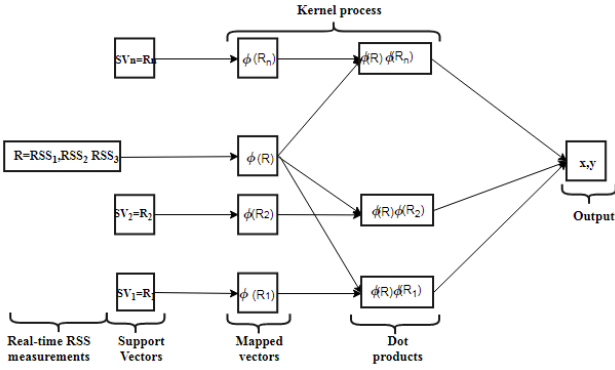


Fig. 4. SVR PD Localisation model

The vector  $R_i = [r_i^1, r_i^2, r_i^3]$  is taken as the SVR input feature vector and used to infer the location  $l_i(x_i, y_i)$ . All the feature vectors from known locations and their corresponding location coordinates constitute the SVR training sample set. Using this training set, the SVR is trained to build a PD localisation models that would subsequently be used to predict or estimate PD location given RSS vector. During training, the input features (RSS) from each known location are transformed to a new feature space with N features, one for each support vector. That is to say that, they are represented only in terms of their dot products with support vectors (special data points chosen by the SVR optimisation algorithm). Gaussian kernel function is employed in the transformation to provide a nonlinear mapping from the input space to the new feature space. In the location estimation phase, for a given RSS vector the kernel finds the similarity or a distance measure between the vector and the support vectors stored after training. The corresponding coordinates of the support vectors closest to the RSS vector are used to compute the PD location for the given RSS vector. The SVR PD location model is as shown in Fig. 4.

However, when the electromagnetic environment changes due to external influences, for example change in the location of an electrical equipment, the localisation model would be retrained by the latest collected data. The retraining process can be done automatically, triggered by the location error analysis. If the location error exceeds a predefined threshold, the retraining begins.

The optimal combination of the RBF kernel based SVR hyper-parameters (kernel parameter, insensitive loss function and regularisation parameter) is obtained via cross validation/grid search method.

### 3.2.2 Least Squares Support Vector Regression:

Least squares support vector regression (LSSVR) algorithm [32] [39] is a reformulation of the standard SVR algorithm described in section 3.2.1.1, which leads to solving a system of linear equations. The idea of linear equations makes LSSVR more appealing and computationally more

economical compare to solving the convex quadratic programming (QP) for standard SVR. LSSVR algorithm for PD localisation consist of two phases: Training and Localisation. During the training phase, the parameters of LSSVR algorithm are estimated using PD measurements at known locations (training points). In the localisation phase, PD measurements taken at unknown locations are analysed, and their locations obtained using the parameters estimated in the training phase. Given a training data set  $\{(r_1, l_1), (r_2, l_2), \dots, (r_n, l_n)\} \subset \mathfrak{R}^n \times \mathfrak{R}$  of n points, with PD input (RSS) data  $r_i \in \mathfrak{R}^n$ , and output (PD location coordinate) data  $l_i(x_i, y_i) \in \mathfrak{R}^2$  in 2-dimension, the LSSVR based PD location optimisation problem in the primal weight space is formulated as:

$$\min_{w, b, e} J(w, e) = \frac{1}{2} \|w\|^2 + \frac{1}{2} \gamma \sum_{i=1}^n e_i^2 \quad (9)$$

s.t

$$l_i = \langle w, \Phi(r_i) \rangle + b + e_i, \quad i = 1, \dots, n$$

with  $\varphi(\cdot): \mathfrak{R}^n \rightarrow \mathfrak{R}^{n_h}$  a function which non-linearly map the input space into the so-called higher dimensional feature space, weight vector  $w \in \mathfrak{R}^{n_h}$  in primal weight space, bias term b and error variable  $e_k \in \mathfrak{R}$ . The error term here represents the true deviation between actual PD location and estimated location, rather than a slack variable which is needed to ensure feasibility (as in SVR case).  $\gamma \geq 0$  is a regularisation constant.

To solve the optimisation problem in the dual space, one defines the Lagrangian

$$L(w, b, e; \alpha) = J(w, e) - \sum_{i=1}^n \alpha_i \{w^T \Phi(r_i) + b + e_i - l_i\} \quad (10)$$

with Lagrange multipliers  $\alpha_i \in \mathfrak{R}$ . The conditions for optimality are given by

$$\left\{ \begin{array}{l} \frac{\partial L_{LS-SVR}}{\partial w} = 0 \rightarrow w = \sum_{i=1}^n \alpha_i \Phi(r_i) \\ \frac{\partial L_{LS-SVR}}{\partial b} = 0 \rightarrow \sum_{i=1}^n \alpha_i = 0 \\ \frac{\partial L_{LS-SVR}}{\partial e_i} = 0 \rightarrow \alpha_i = \gamma e_i \\ \frac{\partial L_{LS-SVR}}{\partial \alpha_i} = 0 \rightarrow \langle w, \Phi(r_i) \rangle + b + e_i - l_i = 0 \end{array} \right. \quad (11)$$

After eliminating w and e, the solution yields the following linear equations:

$$\begin{bmatrix} 0 & 1_v^T \\ 1_v & \Omega + \frac{1}{\gamma} I \end{bmatrix} \begin{bmatrix} b \\ \alpha \end{bmatrix} = \begin{bmatrix} 0 \\ l \end{bmatrix} \quad (12)$$

where  $l = (l_1, \dots, l_n)^T$ ,  $1_v = (1, \dots, 1)^T$  and  $\alpha = (\alpha_1, \dots, \alpha_n)^T$  the Lagrange multipliers. Applying

Mercer's condition [32], the  $ik$ -th element of  $\Omega$  is given by  $\Omega_{ik} = \Phi(r_i)^T \Phi(r_k) = K(r_i, r_k)$   $i, k = 1, \dots, n$ , where  $\Omega$  is a positive definite matrix and  $ik$ -th element of the matrix  $\Omega_{ik} = K(r_i, r_k)$  is a symmetric, continuous function. The resulting LSSVR model for PD location estimation becomes:

$$f(r_i) = \sum_{i=1}^n \alpha_i K(r_i, r) + b \quad (13)$$

where  $\alpha, b$  are obtained during the training phase by solving (10). In LSSVR, there are only two parameters to be tuned: the kernel setting and the regularisation constant. Cross-validation/grid search is used to determine the optimal combination of the parameters.

## 4. Experimental Procedure

### 4.1 Experimental Set Up

In order to verify the effectiveness of the PD localisation system that is based on the deployment of a network of sensor nodes, a systematic test experiment was conducted in a 19.20m x 8.40m laboratory at the University of Strathclyde.

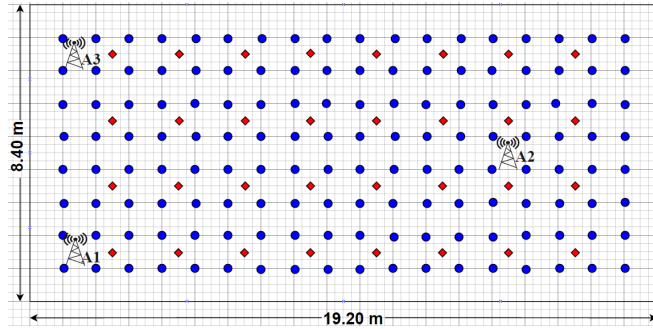


Fig. 5. Measurement grid for measurement campaign

The laboratory contained a great deal of clutter including metallic objects which gives rise to a multipath rich radio environment. Within the accessible area of the laboratory, 144 distinct training locations and 32 testing locations were uniformly selected to form a grid such that the spacing between adjacent training locations is 1 m and the spacing between a training location and its nearest testing location is 0.7 m which represent an array of sensor nodes. Pulse emulated PD sources were set up and 20 RF PD measurements collected at each training and testing location, resulting in 2880 training and 640 testing cases. In real life however, the electrical equipment in which PDs are most likely to appear are not evenly arranged in substations and moreover some areas may be inaccessible. Signal strength decays as the transmission distance increases. This signal propagation characteristic in conjunction with an interpolation algorithm can be explored to automatically estimate PD signal strength at unobserved locations based on the known data values. The duration and the repetition frequency of the discharge pulses were 10ps and 100 kHz respectively. Three omnidirectional antennas used for

capturing the RF signals were deployed at predefined locations. The arrangement of this procedure is shown in Fig. 5. A high-speed multichannel oscilloscope with memory function was used as a signal-acquisition system to capture and store the PD traces. The oscilloscope has a bandwidth of 9GHz. The PD data acquired from measurement were sampled at 2GS/s. A sample waveform of the received PD signals is shown in Fig. 6. The injected PD pulse waveform and the sensor response are shown in Fig. 7.

### 4.2 Data Preparation

RF signals collected during the measurement campaign are corrupted by noise/interference and this needs to be removed before the PD signals are analysed. In this work, the process of noise removal is accomplished using a wavelet multivariate de-noising technique [6]. This de-noising scheme combines the decomposition of information given by wavelet transform and the ability of decorrelation among variables given by the Principal Component Analysis (PCA) [40]. The objective is to obtain better de-noised data so as to extract meaningful information from the raw data for PD location. The energy (defined here as the signal strength) contained in each PD trace is then calculated. The average of the 20 individual measurements taken at each training and test locations is computed. Fig. 8 shows PD signal strength variation with respect to location for each of the antennas. The unique signatures created by PD signal strength at different locations facilitate the application of machine learning algorithms for PD localisation. In order to provide more robustness to our system, the ratio of the averaged signal strength components between pairs of receiving antennas is computed and used as fingerprint input vectors to the developed models.

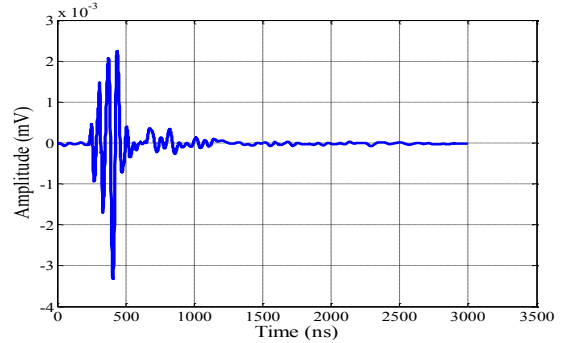


Fig. 6. Recorded PD signal

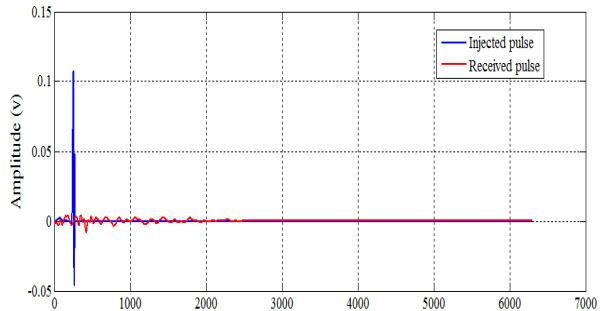


Fig. 7. Response of the receiver sensor for the injected PD pulse



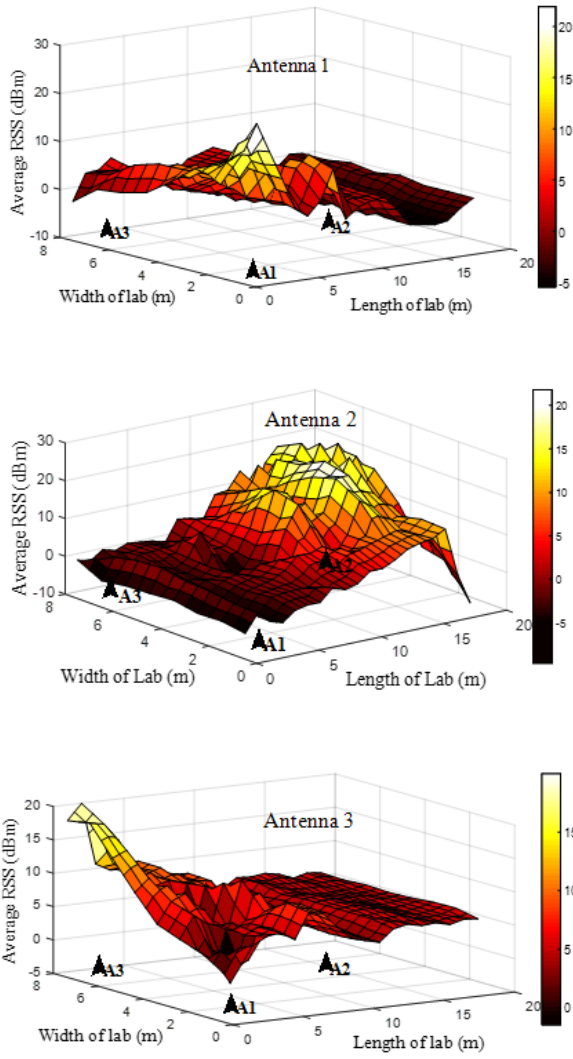


Fig. 8. Spatial variation of RSS for each antenna

## 5. Results and Discussions

The performance of SVM-based models (SVR and LSSVR) on the PD data collected is presented and compared with the ANN method. The empirical evaluation of the models is based on statistical operators of location error as well as their cumulative distribution functions (CDFs).

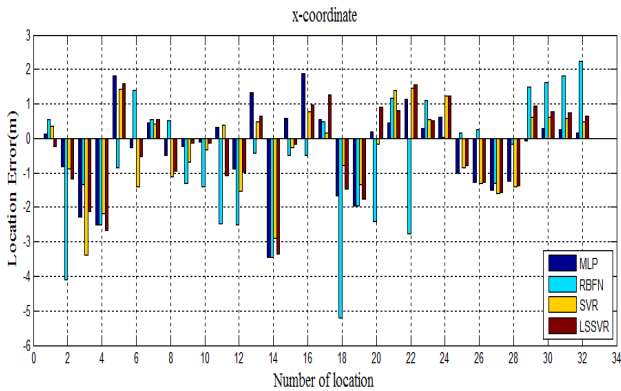


Fig. 9. Model localisation error in x-coordinate

The localisation error is computed as the Euclidean distance between the true location and the estimated location of the PD source. CDF describes the probability of locating PD within a specify range of localisation error. This shows how consistent the models perform and capture both the accuracy and precision of the models.

Fig. 9 and Fig. 10 show the errors in each coordinate (x and y) of the test locations for the three models. This result shows that the location errors in x and y vary from -3.5 m to 1.9 m and -3.7 m to 3.7 m respectively for the MLP model and from -5.2 m to 2.3 m in x and -3.9 m to 3.6 m in y for RBFN. For SVR model, the errors in x and y vary from -3.4 m to 1.5 m and -3.7 m to 2.9 m respectively. The result for LSSVR model is similar to that for the other models with errors in x and y varying from -3.3 m to 1.5m and -3.9 m to 3.3 m respectively. It is observed that the overall accuracy of each of the models will be affected mostly by the y-coordinate predictions.

Fig. 11 shows the localisation error in Euclidean distance for each test location. The maximum localisation error for MLP, RBFN, SVR and LSSVR models is found to be 3.90 m, 6.20 m, 4.5 m and 3.99 m respectively with LSSVR model producing location estimate with the lowest error of 0.2 m.

Fig. 12 shows CDFs of localisation error for the models. The LSSVR model has a precision of 72 % within 2.5 m compare to SVR, RBFN and MLP models with precision of 69 %, 54% and 60 % within 2.5 m respectively. In other words, the localisation error is less than 2.5 m with probability of 72 %, 69 %, 54% and 60 % for LSSVR, SVR, RBFN and MLP respectively.

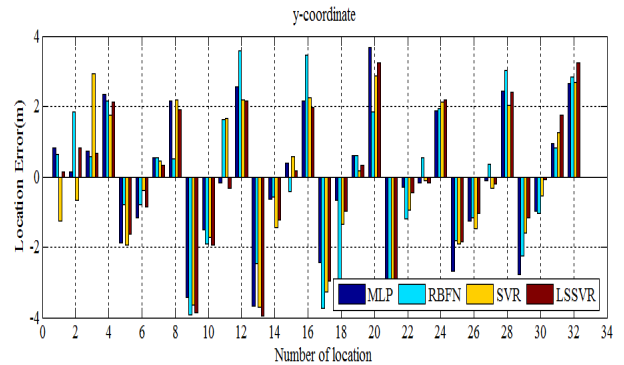


Fig. 10. Model localisation error in y-coordinate

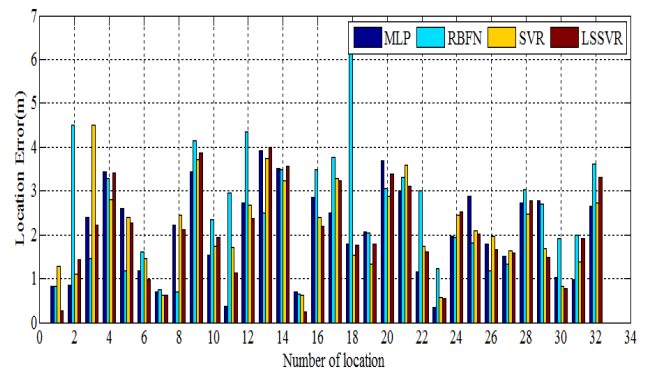


Fig. 11. Model localisation errors

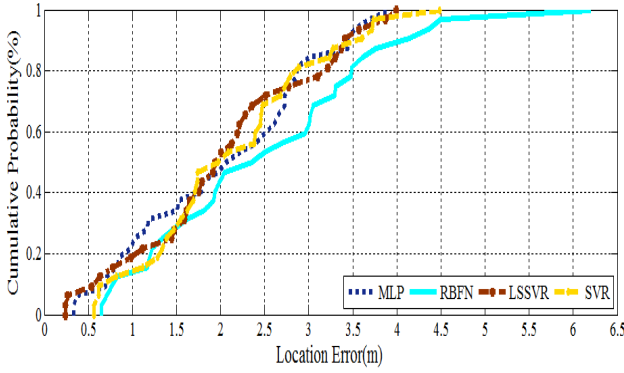


Fig. 12. CDF of model localization errors

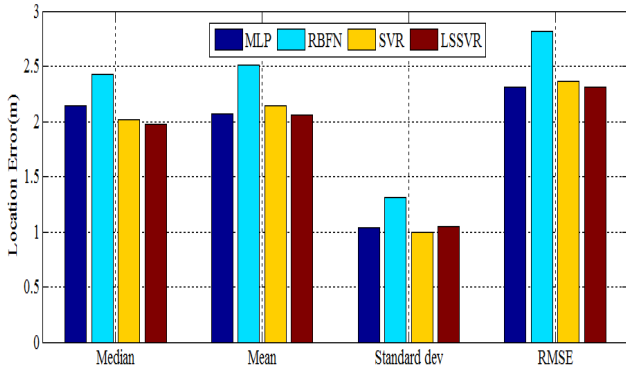


Fig. 13. Model location accuracy

Table 1. Cumulative error probability of model location error

	MLP	RBFN	SVR	LSSVR
CEP=0.25	1.09	1.40	1.43	1.46
CEP=0.50	2.14	2.43	2.03	1.97
CEP=0.75	2.83	3.39	2.76	2.94

Comparison of the performance of the models based on localisation error corresponding to 0.25, 0.50, and 0.75 overall cumulative error probabilities (CEP) is presented in Table 1. This clearly shows that half of the time PD sources were located with error less than 2 m when LSSVR algorithm is used for localisation.

The results of localisation accuracy for the models are shown in Fig. 13. It is clear that there is a steady improvement in location accuracy in terms of median error when the SVM-based models are used compared to ANN models. LSSVR model particularly shows an 8.32 % and 22.8 % reduction in median location error when compared with MLP and RBFN models respectively.

## 6. Conclusion

Machine learning technique for locating PD sources based on RSS measurement have been considered. The principle and computational realisation of the methods based on support vector machine have been described. Support vector regression (SVR) as well as least squares support vector regression (LSSVR) approach uses the spatial pattern of received signal strength to construct a regression surface in a high dimensional feature space where PD location is determined. This approach models PD location as a linear

combination of RSS measurement. In this study, signal strength ratio is used as location fingerprints rather than absolute RSS. The performance of the proposed methods have been evaluated and compared with ANN in terms of statistical operators of localisation error. The results indicate that SVM-based approaches are superior to ANN in accuracy showing a reduction in median location error and represent practical alternatives for PD source localisation. It is believed that the superior performance of SVM-based approaches is due to their ability to converge to a global minimum whereas neural networks are susceptible to converging to local minima. Given the rich complexity of the underlying radio environment convergence to a local minima is highly likely; therefore, SVM-based approaches are more appropriate in this environment. This PD localisation system can monitor and locate discharges from several items of plant concurrently making it suitable for substation-wide PD localisation.

## 7. Acknowledgments

The authors acknowledge the Engineering and Physical Sciences Research Council for their support of this work under grant EP/J015873/1 and Tertiary Education Trust Fund (TETFund) Nigeria.

## 8. References

- [1] H. Hou, G. Sheng, and X. Jiang, "Localization algorithm for the PD source in substation based on L-shaped antenna array signal processing," *IEEE Transactions on Power Delivery*, vol. 30, no. 1, pp. 472--479, 2015.
- [2] H. A. Iliias, M. A. Tunio, A. H. A. Bakar, H. Mokhlis, and G. Chen, "Partial discharge phenomena within an artificial void in cable insulation geometry: experimental validation and simulation," *IEEE Transactions on Dielectrics and Electrical Insulation*, vol. 23, no. 1, pp. 451--459, 2016.
- [3] R. Rostaminia, M. Saniei, M. Vakilian, S. S. Mortazavi and V. Parvin, "Accurate power transformer PD pattern recognition via its model," *IET Science, Measurement Technology*, vol. 10, no. 7, pp. 745-753, 2016.
- [4] P. J. Moore, I. E. Portugues, and I. A. Glover, "Partial discharge investigation of a power transformer using wireless wideband radio-frequency measurements," *IEEE Transactions on Power Delivery*, vol. 21, no. 1, pp. 528--530, 2006.
- [5] F. P. Mohamed, W.H. Siew and J.J. Soraghan, "Online partial discharge detection in medium voltage cables using protection and instrument current transformers," *Second UHVNet Colloquium on high voltage measurement and insulation research*, Glasgow, 2009.
- [6] D. Evagorou, A. Kyprianou, P.L. Lewin, A. Stavrou, V. Efthymiou, A.C. Metaxas, and G.E. Georghiou, "Feature extraction of partial discharge signals using the wavelet packet transform and classification with a probabilistic neural network," *IET Science, Measurement & Technology*, vol. 4, no. 3, pp. 177-192, 2010.
- [7] Y. Lu, X. Tan and X. Hu, "PD detection and localisation by acoustic measurements in an oil-filled transformer," *IEE Proceedings - Science, Measurement and Technology*, vol. 147, no. 2, pp. 81-85, 2000.
- [8] P Li, W Zhou, S Yang, Y Liu, Y Tian and Y Wang, "Method for partial discharge localisation in air-insulated substations," *IET Science, Measurement & Technology*, 2017.
- [9] F. P. Mohamed, W. H. Siew, J. J. Soraghan, S. M. Strachan and J. McWilliam, "Remote monitoring of partial discharge data from insulated power cables," *IET Science, Measurement Technology*, vol. 8, no. 5, pp. 319-326, 2014.
- [10] I. E. Portugues, P. J. Moore, I. A. Glover, C. Johnstone, R. H. McKosky, M. B. Goff, and L. Van Der Zel, "RF-based partial discharge early warning system for air-insulated substations," *IEEE Transactions on Power Delivery*, vol. 24, no. 1, pp. 20--29, 2009.



- [11] H. Hou, G. Sheng, P. Miao, X. Li, Y. Hu, and X. Jiang, "Partial discharge location based on radio frequency antenna array in substation," *High Voltage Engineering*, vol. 38, no. 6, pp. 1334-1340, 2012.
- [12] J. Tang and Y. Xie, "Partial discharge location based on time difference of energy accumulation curve of multiple signals," *IET Electric Power Applications*, vol. 5, no. 1, pp. 175-180, 2011.
- [13] H. Hou, G. Sheng and X. Jiang, "Robust Time Delay Estimation Method for Locating UHF Signals of Partial Discharge in Substation," *IEEE Transactions on Power Delivery*, vol. 28, no. 3, pp. 1960-1968, 2013.
- [14] M. D. Judd, "Radiometric partial discharge detection," *International Conference on Condition Monitoring and Diagnosis*, Beijing, 2008.
- [15] I. E. Portugues, P. J. Moore and P. Carder, "The use of radiometric partial discharge location equipment in distribution substations," *18th International Conference and Exhibition on Electricity Distribution*, Turin, 2005.
- [16] M. X. Zhu, Y. B. Wang, Q. Liu, J. N. Zhang, J. B. Deng, G. J. Zhang, X. J. Shao and W. L. He, "Localization of multiple partial discharge sources in air-insulated substation using probability-based algorithm," *IEEE Transactions on Dielectrics and Electrical Insulation*, vol. 24, no. 1, pp. 157-166, 2017.
- [17] R. A. Hooshmand, M. Parastegari and M. Yazdanpanah, "Simultaneous location of two partial discharge sources in power transformers based on acoustic emission using the modified binary partial swarm optimisation algorithm," *IET Science, Measurement Technology*, vol. 7, no. 2, pp. 112-118, 2013.
- [18] C. Boya, M. V. Rojas-Moreno, M. Ruiz-Llata, and G. Robles, "Location of partial discharges sources by means of blind source separation of UHF signals," *IEEE Transactions on Dielectrics and Electrical Insulation*, vol. 22, no. 4, pp. 2302--2310, 2015.
- [19] H. H. Sinaga, B. T. Phung, and T. R. Blackburn, "Partial discharge localization in transformers using UHF detection method," *IEEE Transactions on Dielectrics and Electrical Insulation*, vol. 19, no. 6, pp. 1891--1900, 2012.
- [20] E. T. Iorkyase and C. Tachtatzis and R. C. Atkinson and I. A. Glover, "Localisation of partial discharge sources using radio fingerprinting technique," *Loughborough Antennas Propagation Conference (LAPC)*, Loughborough, 2015.
- [21] D. Genming and J. Zhang, L. Zhang, and Z. Tan, "Overview of received signal strength based fingerprinting localization in indoor wireless LAN environments," *IEEE 5th International Symposium on Microwave, Antenna, Propagation and EMC Technologies for Wireless Communications (MAPE)*, 2013.
- [22] P. J. Chuang and Y. J. Jiang, "Effective neural network-based node localisation scheme for wireless sensor networks," *IET Wireless Sensor Systems*, vol. 4, no. 2, pp. 97-103, 2014.
- [23] J. Roj, "Estimation of the artificial neural network uncertainty used for measurand reconstruction in a sampling transducer," *IET Science, Measurement Technology*, vol. 8, no. 1, pp. 23-29, 2014.
- [24] S. Mohanty and S. Ghosh, "Artificial neural networks modelling of breakdown voltage of solid insulating materials in the presence of void," *IET Science, Measurement Technology*, vol. 4, no. 5, pp. 278-288, 2010.
- [25] C. Laoudias, P. Kemppi, and C. G. Panayiotou, "Localization using radial basis function networks and signal strength fingerprints in WLAN," *IEEE Global telecommunications conference, 2009.*, Honolulu, 2009.
- [26] C. Nerguizian, C. Despins, and S. Affes, "Indoor geolocation with received signal strength fingerprinting technique and neural networks," *International Conference on Telecommunications*, Berlin, 2004.
- [27] E. Jiang, P. Zan, X. Zhu, J. Liu and Y. Shao, "Rectal sensation function rebuilding based on optimal wavelet packet and support vector machine," *IET Science, Measurement Technology*, vol. 7, no. 3, pp. 139-144, 2013.
- [28] L. Hao, and P. L. Lewin, "Partial discharge source discrimination using a support vector machine," *IEEE Transactions on Dielectrics and Electrical Insulation*, vol. 17, no. 1, pp. 189--197, 2010.
- [29] B. Ravikumar, D. Thukaram and H. P. Khincha, "Application of support vector machines for fault diagnosis in power transmission system," *IET Generation, Transmission Distribution*, vol. 2, no. 1, pp. 119-130, 2008.
- [30] Y. Khan, A. A. Khan, F. N. Budiman, A. Beroual, N. H. Malik, and A. A. Al-Arainy, "Partial discharge pattern analysis using support vector machine to estimate size and position of metallic particle adhering to spacer in GIS," *Electric Power Systems Research*, vol. 116, pp. 391--398, 2014.
- [31] A. Ben-Hur, D. Horn, H. T. Siegelmann, and V. Vapnik, "Support vector clustering," *The Journal of Machine Learning Research*, vol. 2, pp. 125--137, 2002.
- [32] S. A. Bessedik and H. Hadi, "Prediction of flashover voltage of insulators using least squares support vector machine with particle swarm optimisation," *Electric Power Systems Research*, vol. 104, pp. 87-92, 2013.
- [33] D. Basak, S. Pal, and D. C. Patranabis, "Support vector regression," *Neural Information Processing-Letters and Reviews*, vol. 11, no. 10, pp. 203--224, 2007.
- [34] H. R. Zhang, X. D. Wang, C. J. Zhang and X. S. Cai, "Robust identification of non-linear dynamic systems using support vector machine," *IEE Proceedings - Science, Measurement and Technology*, vol. 153, no. 3, pp. 125-129, 2006.
- [35] S. M. Clarke, J. H. Griebisch, and T. W. Simpson, "Analysis of support vector regression for approximation of complex engineering analyses," *Journal of mechanical design*, vol. 127, no. 6, pp. 1077--1087, 2005.
- [36] K. Shi, Z. Ma, R. Zhang, W. Hu, and H. Chen, "Support Vector Regression Based Indoor Location in IEEE 802.11 Environments," *Mobile Information Systems*, vol. 2015, p. 14, 2015.
- [37] K. P. Bennett, and C. Campbell, "Support vector machines: hype or hallelujah?," *ACM SIGKDD Explorations Newsletter*, vol. 2, no. 1, pp. 1-13, 2000.
- [38] M. Junshui, T. James and P. Simon, "Accurate On-line Support Vector Regression," *Neural Computation*, vol. 15, no. 11, pp. 2683--2703, 2003.
- [39] Z. Wu, C. Li, Z. Yang, and P. Wang, "Research on tourists' positioning technology based on LSSVR," *IEEE Advanced Information Technology, Electronic and Automation Control Conference*, Chongqing, 2015.
- [40] S. Mohanty, K. K. Gupta and K. S. Raju, "Adaptive fault identification of bearing using empirical mode decomposition-principal component analysis-based average kurtosis technique," *IET Science, Measurement Technology*, vol. 11, no. 1, pp. 30-40, 2017.